Matter profile effect in a neutrino factory

T. Ota
Department of Physics, Kyushu University, Fukuoka 812-8581, Japan

J. Sato
Research Center for Higher Education, Kyushu University, Ropponmatsu, Chuo-ku, Fukuoka, 810-8560, Japan

(Received 21 November 2000; published 9 April 2001)

We point out that the matter profile effect—the effect of matter density fluctuation on the baseline—is very important to estimate the parameters in a neutrino factory with a very long baseline. To make it clear, we propose the method of Fourier series expansion of the matter profile. By using this method, we can take account of both the matter profile effect and its ambiguity. For very long baseline experiment, such as $L = 7332$ km, in the analysis of the oscillation phenomena we need to introduce a new parameter a_1—the Fourier coefficient of the matter profile—as a theoretical parameter to deal with the matter profile effects.

DOI: 10.1103/PhysRevD.63.093004 PACS number(s): 14.60.Pq, 11.30.Er, 13.15.+g

I. INTRODUCTION

Evidence of neutrino oscillations was presented by the Super-Kamiokande Collaboration [1]. Many experiments have been planned and some of them have already been carried out to determine the parameters of neutrino oscillation [2]. Recently, the neutrino factory [3]—a very long (over 1000 km) baseline experiment with high-energy neutrinos from a muon storage ring—has been proposed as the most effective experiment to determine the unknown parameters U_{e3}, the sign of Δm^2 that is responsible for the atmospheric neutrino anomaly and the *CP* violating phase [4–13].

To analyze the oscillation phenomena with such a long baseline, we have to treat the matter effect [14] very carefully. Two ways have been adopted to deal with matter effects: (i) to add the averaged matter density $\overline{\rho}$ as a parameter in addition to the other theoretical parameters such as the mixing angles, and estimate it in the same way as the other parameters [5,9,11]; (ii) to use the preliminary reference Earth model [15] (PREM) for the matter density profile, and to assume that we know the ingredients of the Earth completely [4,6]. We have, however, questions about these treatments. For method (i), we ask, ''Can we describe the matter effect precisely enough by only averaged matter density?'' The answer is ''No, we cannot. Sometimes the deviation from the constant density is important.'' [4].

For method (ii), we ask ''Is the PREM a trustworthy model for neutrino oscillation experiments?'' The PREM was originally based on the study of earthquake waves; hence it predicts the density profile in the depth. However, it does not predict the ingredients of matter. Therefore, there is an ambiguity in electron number fraction. Then, we should worry about possible ambiguities in electron number density. If we estimated the parameters without considering their ambiguity, we would have significant errors in the estimates for the parameters. Therefore, we must introduce a way to take into account the matter profile effect as the parameter determined by the experiments. We propose the method of the Fourier series expansion of the matter profile [16]. Using the Fourier expansion we can parametrize the matter profile. We can express the matter profile effect with a finite number of parameters by examining how many terms of the Fourier expansion contribute to the oscillation physics within the resolution of the experiments. We can incorporate the matter profile's ambiguity in the ambiguities of the Fourier coefficients.

We will review the method of the Fourier series and investigate qualitatively the circumstances that make the matter profile effect relevant in Sec. II. In Sec. III, we will calculate quantitatively the oscillation probabilities and the event rates with various sets of the parameters in baseline lengths.

II. THE METHOD OF THE FOURIER SERIES

In this section we introduce the Fourier expansion method. First, we describe its formalism and see its feature. Then, we solve the evolution equation for neutrinos in matter perturbatively, and study the condition where the matter profile effect is significant.

A. Fourier expansion method

Assuming three generations of neutrinos, we parametrize the lepton mixing matrix

$$U_{\alpha i} \equiv e^{i\psi\lambda_7}\Gamma e^{i\phi\lambda_5}e^{i\omega\lambda_2}U_{\text{Majorana}} \tag{1}$$

$$= \begin{pmatrix} 1 & & \\ & c_\psi & s_\psi \\ & -s_\psi & c_\psi \end{pmatrix} \begin{pmatrix} 1 & & \\ & 1 & \\ & & e^{i\delta} \end{pmatrix} \begin{pmatrix} c_\phi & & s_\phi \\ & 1 & \\ -s_\phi & & c_\phi \end{pmatrix} \begin{pmatrix} c_\omega & s_\omega & \\ -s_\omega & c_\omega & \\ & & 1 \end{pmatrix} U_{\text{Majorana}}$$

$$= \begin{pmatrix} c_\phi c_\omega & c_\phi s_\omega & s_\phi \\ -c_\psi s_\psi - s_\psi s_\phi c_\omega e^{i\delta} & c_\psi c_\omega - s_\psi s_\phi s_\omega e^{i\delta} & s_\psi c_\phi e^{i\delta} \\ s_\psi s_\omega - c_\psi s_\phi c_\omega e^{i\delta} & -s_\psi c_\omega - c_\psi s_\phi s_\omega e^{i\delta} & c_\psi c_\phi e^{i\delta} \end{pmatrix} U_{\text{Majorana}},$$

which relates the flavor eigenstates $|\nu_\alpha\rangle$ $(\alpha = e, \mu, \tau)$ with the mass eigenstates in vacuum $|\nu_i\rangle$ $(i = 1,2,3)$ as

$$|\nu_\alpha\rangle = U_{\alpha i}|\nu_i\rangle. \tag{2}$$

U_{Majorana} is part of the Majorana phases. It does not contribute to the neutrino oscillation phenomena and hence is omitted hereafter.

The evolution in matter of the flavor eigenstates of neutrinos[1] with its energy E is given by

$$i\frac{d}{dx}|\nu_\beta(x)\rangle = H(x)_{\beta\alpha}|\nu_\alpha(x)\rangle, \tag{3}$$

$$H(x)_{\beta\alpha} \equiv \frac{1}{2E}\left\{ U_{\beta i}\begin{pmatrix} 0 & & \\ & \Delta m^2_{21} & \\ & & \Delta m^2_{31} \end{pmatrix} U^\dagger_{i\alpha} + \begin{pmatrix} a(x) & & \\ & 0 & \\ & & 0 \end{pmatrix}_{\beta\alpha} \right\},$$

where

$$\Delta m^2_{ij} \equiv m^2_i - m^2_j,$$

m_i is the mass eigenvalue,

$$a(x) \equiv 2\sqrt{2} G_F n_e(x) E = 7.56 \times 10^{-5} \left(\frac{\rho(x)}{\text{g/cm}^3}\right)\left(\frac{Y_e}{0.5}\right)\left(\frac{E}{\text{GeV}}\right) \text{ eV}^2, \tag{4}$$

where G_F is the Fermi constant, $n_e(x)$ is the electron number density, $\rho(x)$ is the matter density, and Y_e is the electron fraction.

To parametrize the matter effect, $a(x)$, we expand $a(x)$ into a Fourier series as

$$a(x) = \sum_{n=-\infty}^{\infty} a_n e^{-ip_n x}, \quad p_n \equiv \frac{2\pi}{L} n. \tag{5}$$

Note that $a_{-n} = a_n^*$ due to the reality of $a(x)$. Also within the PREM,

$$a_{-n} = a_n \tag{6}$$

since $a(x) = a(L-x)$.

If this expansion can be approximated with a finite number $(\equiv N)$ of terms,

$$a(x) = \sum_{n=-N}^{n=N} a_n e^{-ip_n x}, \tag{7}$$

then it means that the matter profile effect can be parametrized. Thus, by introducing new parameters a_n $(n = -N, \ldots, N)$ [or $n = 0, \ldots, N$, if Eq. (6) holds], we can investigate the oscillation physics without the help of Earth models.

B. Perturbative analysis of the matter profile effect

We solve the evolution equation (3) to see the qualitative feature of the matter profile effect. First, we divide the Hamiltonian $H(x)$ into three pieces for the later calculation:

$$H_{00} \equiv \frac{1}{2E} e^{i\psi\lambda_7} \Gamma \begin{pmatrix} \Delta m^2_{31} s^2_\phi + \overline{a} + \Delta m^2_{21} c^2_\phi s^2_\omega & 0 & \Delta m^2_{31} c_\phi s_\phi - \Delta m^2_{21} c_\phi s_\phi s^2_\omega \\ 0 & \Delta m^2_{21} c^2_\omega & 0 \\ \Delta m^2_{31} c_\phi s_\phi - \Delta m^2_{21} c_\phi s_\phi s^2_\omega & 0 & \Delta m^2_{31} c^2_\phi + \Delta m^2_{21} s^2_\phi s^2_\omega \end{pmatrix} \Gamma^\dagger e^{-i\psi\lambda_7}, \tag{8}$$

$$H_{01} \equiv \frac{\Delta m^2_{21}}{2E} c_\omega s_\omega e^{i\psi\lambda_7} \Gamma \begin{pmatrix} 0 & c_\phi & 0 \\ c_\phi & 0 & -s_\phi \\ 0 & -s_\phi & 0 \end{pmatrix} \Gamma^\dagger e^{-i\psi\lambda_7}, \tag{9}$$

$$H_1(x) \equiv \frac{1}{2E}\begin{pmatrix} \delta a(x) & & \\ & 0 & \\ & & 0 \end{pmatrix}, \tag{10}$$

[1]For antineutrinos $a(x)$ and δ should be replaced by $-a(x)$ and $-\delta$.

where $\bar{a} \equiv a_0$ and $\delta a(x) \equiv a(x) - \bar{a}$. The oscillation phenomena arise from H_{00}; hence its effect must be fully taken into account. On the other hand, H_{01} and $H_1(x)$ can be treated as the perturbation in almost all cases in neutrino factories, since

$$\left| \frac{\Delta m_{21}^2 L}{2E} \right| \ll 1, \quad \left| \frac{\delta a(x) L}{2E} \right| \ll 1 \tag{11}$$

can be almost always expected. Note that we have to include Δm_{21}^2 terms in $(H_{00})_{ij}$ $(i,j=1,3)$ to deal with the resonance effect.[2]

Next, we rewrite H_{00} as

$$H_{00} = \frac{1}{2E} \tilde{U}_0 \begin{pmatrix} \lambda_- & & \\ & \Delta m_{21}^2 c_\omega^2 & \\ & & \lambda_+ \end{pmatrix} \tilde{U}_0^\dagger, \tag{12}$$

where $\tilde{U}_0$ and $\lambda_\pm$ are the mixing matrix and mass square eigenvalues in matter up to the zeroth order of the ''perturbation'' H_{01} and $H_1(x)$ and are defined by

$$\tilde{U}_0 \equiv e^{i\psi\lambda_7} \Gamma e^{i\tilde{\phi}\lambda_5} = \begin{pmatrix} c_{\tilde{\phi}} & 0 & s_{\tilde{\phi}} \\ -s_\psi s_{\tilde{\phi}} e^{i\delta} & c_\psi & s_\psi c_{\tilde{\phi}} e^{i\delta} \\ -c_\psi s_{\tilde{\phi}} e^{i\delta} & s_\psi & c_\psi c_{\tilde{\phi}} e^{i\delta} \end{pmatrix}, \tag{13}$$

$$\tan 2\tilde{\phi} = \frac{s_{2\phi}(\Delta m_{31}^2 - \Delta m_{21}^2 s_\omega^2)}{c_{2\phi}(\Delta m_{31}^2 - \Delta m_{21}^2 s_\omega^2) - \bar{a}}, \tag{14}$$

$$\lambda_\pm = \frac{1}{2}\{\alpha \pm \beta\}, \tag{15}$$

$$\alpha \equiv \Delta m_{31}^2 + \Delta m_{21}^2 s_\omega^2 + \bar{a},$$

$$\beta \equiv \sqrt{\{(\Delta m_{31}^2 - \Delta m_{21}^2 s_\omega^2) c_{2\phi} - \bar{a}\}^2 + (\Delta m_{31}^2 - \Delta m_{21}^2 s_\omega^2)^2 s_{2\phi}^2}.$$

Then we solve the evolution equation (3) perturbatively as

$$\begin{aligned} |\nu_\beta(L)\rangle &= T\left[\exp\left(-i \int_0^L H(x) dx \right) \right]_{\beta\alpha} |\nu_\alpha(0)\rangle \\ &= \left(e^{-iH_{00}L} + e^{-iH_{00}L}(-i) \int_0^L H_{01I} dx + e^{-iH_{00}L}(-i) \int_0^L H_1(x)_I dx + \cdots \right)_{\beta\alpha} |\nu_\alpha(0)\rangle \\ &\equiv (S_{00} + S_{01} + S_1 + \cdots)_{\beta\alpha} |\nu_\alpha(0)\rangle, \end{aligned} \tag{16}$$

where S_{00}, S_{01}, and S_1 are defined by the first, second, and third terms in the second line, respectively. S_{01} and S_1 are the perturbative contributions at the first order from H_{01} and H_1 respectively. S_{00}, S_{01}, and S_1 are calculated to be

[2]On the other hand, we include the Δm_{21}^2 term in the (22) element just for convenience. This inclusion is not essential.

$$
\begin{aligned}
S_{00}(L)_{\beta\alpha} &\equiv e^{-iH_{00}L} \\
&= \tilde{U}_0 \begin{pmatrix} e^{-i(\lambda_-/2E)L} & & \\ & e^{-i(\Delta m^2_{21}c^2_\omega/2E)L} & \\ & & e^{-i(\lambda_+/2E)L} \end{pmatrix} \tilde{U}_0^\dagger \\
&= \begin{pmatrix} S^2_{\tilde{\phi}} e^{-i(\lambda_+/2E)L} + c^2_{\tilde{\phi}} e^{-i(\lambda_-/2E)L} & \frac{1}{2} e^{-i\delta} s_\psi s_{2\tilde{\phi}} (e^{-i(\lambda_+/2E)L} - e^{-i(\lambda_-/2E)L}) & \\ \frac{1}{2} e^{i\delta} s_\psi s_{2\tilde{\phi}} (e^{-i(\lambda_+/2E)L} - e^{-i(\lambda_-/2E)L}) & s^2_\psi (c^2_{\tilde{\phi}} e^{-i(\lambda_+/2E)L} + s^2_{\tilde{\phi}} e^{-i(\lambda_-/2E)L}) + c^2_\psi e^{-i(\Delta m^2_{21}c^2_\omega/2E)L} & \\ \frac{1}{2} e^{i\delta} s_\psi s_{2\tilde{\phi}} (e^{-i(\lambda_+/2E)L} - e^{-i(\lambda_-/2E)L}) & \frac{1}{2} s_{2\psi} (c^2_{\tilde{\phi}} e^{-i(\lambda_+/2E)L} + s^2_{\tilde{\phi}} e^{-i(\lambda_-/2E)L} - e^{-i(\Delta m^2_{21}c^2_\omega/2E)L}) & \end{pmatrix} \\
&\qquad \begin{pmatrix} \frac{1}{2} e^{i\delta} c_\psi s_{2\tilde{\phi}} (e^{-i(\lambda_+/2E)L} - e^{-i(\lambda_-/2E)L}) \\ \frac{1}{2} s_{2\psi} (c^2_{\tilde{\phi}} e^{-i(\lambda_+/2E)L} + s^2_{\tilde{\phi}} e^{-i(\lambda_-/2E)L} - e^{-i(\Delta m^2_{21}c^2_\omega/2E)L}) \\ c^2_\psi (c^2_{\tilde{\phi}} e^{-i(\lambda_+/2E)L} + s^2_{\tilde{\phi}} e^{-i(\lambda_-/2E)L}) + s^2_\psi e^{-i(\Delta m^2_{21}c^2_\omega)/2E} \end{pmatrix}, \qquad (17)
\end{aligned}
$$

$$
\begin{aligned}
S_{01}(L)_{\beta\alpha} &\equiv e^{-iH_{00}L}(-i)\int_0^L dx H_{01I} = \tilde{U}_0 \begin{pmatrix} 0 & \mathcal{A} & 0 \\ \mathcal{A} & 0 & \mathcal{B} \\ 0 & \mathcal{B} & 0 \end{pmatrix} \tilde{U}_0^\dagger \\
&= \begin{pmatrix} 0 & c_\psi (c_{\tilde{\phi}}\mathcal{A} + s_{\tilde{\phi}}\mathcal{B}) & -s_\psi (c_{\tilde{\phi}}\mathcal{A} + s_{\tilde{\phi}}\mathcal{B}) \\ c_\psi (c_{\tilde{\phi}}\mathcal{A} + s_{\tilde{\phi}}\mathcal{B}) & -s_{2\psi}(s_{\tilde{\phi}}\mathcal{A} - c_{\tilde{\phi}}\mathcal{B}) c_\delta & (e^{i\delta}s^2_\psi - e^{-i\delta}c^2_\psi)(s_{\tilde{\phi}}\mathcal{A} - c_{\tilde{\phi}}\mathcal{B}) \\ -s_\psi (c_{\tilde{\phi}}\mathcal{A} + s_{\tilde{\phi}}\mathcal{B}) & -(e^{i\delta}c^2_\psi - e^{-i\delta}s^2_\psi)(s_{\tilde{\phi}}\mathcal{A} - c_{\tilde{\phi}}\mathcal{B}) & s_{2\psi}(s_{\tilde{\phi}}\mathcal{A} - c_{\tilde{\phi}}\mathcal{B}) c_\delta \end{pmatrix}, \qquad (18)
\end{aligned}
$$

$$
\mathcal{A} \equiv \frac{\Delta m^2_{21}}{2(\Delta m^2_{21}c^2_\omega - \lambda_-)} c_{\phi-\tilde{\phi}} s_{2\omega} (e^{-i(\Delta m^2_{21}c^2_\omega/2E)L} - e^{-i(\lambda_-/2E)L}), \qquad (19)
$$

$$
\mathcal{B} \equiv \frac{\Delta m^2_{21}}{2(\lambda_+ - \Delta m^2_{21}c^2_\omega)} s_{\phi-\tilde{\phi}} s_{2\omega} (e^{-i(\Delta m^2_{21}c^2_\omega/2E)L} - e^{-i(\lambda_+/2E)L}), \qquad (20)
$$

$$
\begin{aligned}
S_1(L)_{\beta\alpha} &\equiv e^{-iH_{00}L}(-i)\int_0^L dx H_1(x)_I = \sum_n \tilde{U}_0 \begin{pmatrix} 0 & 0 & \mathcal{C}_n \\ 0 & 0 & 0 \\ \mathcal{D}_n & 0 & 0 \end{pmatrix} \tilde{U}_0^\dagger \\
&= \sum_n \begin{pmatrix} (\mathcal{C}_n + \mathcal{D}_n) s_{\tilde{\phi}} c_{\tilde{\phi}} & e^{-i\delta} s_\psi (-\mathcal{D}_n s^2_{\tilde{\phi}} + \mathcal{C}_n c^2_{\tilde{\phi}}) & e^{-i\delta} c_\psi (-\mathcal{D}_n s^2_{\tilde{\phi}} + \mathcal{C}_n c^2_{\tilde{\phi}}) \\ e^{i\delta} s_\psi (\mathcal{D}_n c^2_{\tilde{\phi}} + \mathcal{C}_n s^2_{\tilde{\phi}}) & -(\mathcal{C}_n + \mathcal{D}_n) s^2_\psi s_{\tilde{\phi}} c_{\tilde{\phi}} & -(\mathcal{C}_n + \mathcal{D}_n) s_\psi c_\psi s_{\tilde{\phi}} c_{\tilde{\phi}} \\ e^{i\delta} c_\psi (\mathcal{D}_n c^2_{\tilde{\phi}} + \mathcal{C}_n s^2_{\tilde{\phi}}) & -(\mathcal{C}_n + \mathcal{D}_n) s_\psi c_\psi s_{\tilde{\phi}} c_{\tilde{\phi}} & -(\mathcal{C}_n + \mathcal{D}_n) c^2_\psi s_{\tilde{\phi}} c_{\tilde{\phi}} \end{pmatrix} \\
&= \sum_n a_n \frac{s_{2\tilde{\phi}} (e^{-i(\lambda_+/2E)L} - e^{-i(\lambda_-/2E)L})}{2\{(\lambda_+ - \lambda_-)^2 - (2Ep_n)^2\}} \\
&\quad \times \begin{pmatrix} (\lambda_+ - \lambda_-) s_{2\tilde{\phi}} & e^{-i\delta} s_\psi \{(\lambda_+ - \lambda_-) c_{2\tilde{\phi}} - 2Ep_n\} & e^{-i\delta} c_\psi \{(\lambda_+ - \lambda_-) c_{2\tilde{\phi}} - 2Ep_n\} \\ e^{i\delta} s_\psi \{(\lambda_+ - \lambda_-) c_{2\tilde{\phi}} + 2Ep_n\} & -(\lambda_+ - \lambda_-) s^2_\psi s_{2\tilde{\phi}} & -\frac{1}{2}(\lambda_+ - \lambda_-) s_{2\psi} s_{2\tilde{\phi}} \\ e^{i\delta} c_\psi \{(\lambda_+ - \lambda_-) c_{2\tilde{\phi}} + 2Ep_n\} & -\frac{1}{2}(\lambda_+ - \lambda_-) s_{2\psi} s_{2\tilde{\phi}} & -(\lambda_+ - \lambda_-) c^2_\psi s_{2\tilde{\phi}} \end{pmatrix}, \qquad (21)
\end{aligned}
$$

$$\mathcal{C}_n \equiv \frac{a_n}{2(\lambda_+ - \lambda_- + 2Ep_n)} s_{2\tilde{\phi}} (e^{-i(\lambda_+/2E)L} - e^{-i(\lambda_-/2E)L}) = \mathcal{D}_{-n}, \tag{22}$$

$$\mathcal{D}_n \equiv \frac{a_n}{2(\lambda_+ - \lambda_- - 2Ep_n)} s_{2\tilde{\phi}} (e^{-i(\lambda_+/2E)L} - e^{-i(\lambda_-/2E)L}) = \mathcal{C}_{-n}. \tag{23}$$

With Eqs. (17), (18), and (21), the oscillation probability, for example, from ν_e to ν_μ, up to the lowest order of the perturbations, H_{01} and $H_1(x)$, is calculated as

$$\begin{aligned}
P_{\nu_e \to \nu_\mu} &= |S(L)_{\mu e}|^2 \\
&\simeq |(S_{00})_{\mu e}|^2 + 2\,\mathrm{Re}[(S_{00})_{\mu e}(S_{01})^*_{\mu e}] + 2\,\mathrm{Re}[(S_{00})_{\mu e}(S_1)^*_{\mu e}] \\
&= s^2_\psi s^2_{2\tilde{\phi}} \sin^2 \frac{\lambda_+ - \lambda_-}{4E} L + \frac{1}{2} c_\delta s_{2\psi} s_{2\omega} s_{2\tilde{\phi}} \\
&\quad \times \left[\left(c_{\tilde{\phi}} c_{\phi - \tilde{\phi}} \frac{\Delta m^2_{21}}{\Delta m^2_{21} c^2_\omega - \lambda_-} + s_{\tilde{\phi}} s_{\phi - \tilde{\phi}} \frac{\Delta m^2_{21}}{\lambda_+ - \Delta m^2_{21} c^2_\omega} \right) \sin^2 \frac{\Delta m^2_{21} c^2_\omega - \lambda_-}{4E} L \right. \\
&\quad - \left(c_{\tilde{\phi}} c_{\phi - \tilde{\phi}} \frac{\Delta m^2_{21}}{\Delta m^2_{21} c^2_\omega - \lambda_-} + s_{\tilde{\phi}} s_{\phi - \tilde{\phi}} \frac{\Delta m^2_{21}}{\lambda_+ - \Delta m^2_{21} c^2_\omega} \right) \sin^2 \frac{\lambda_+ - \Delta m^2_{21} c^2_\omega}{4E} L \\
&\quad \left. + \left(c_{\tilde{\phi}} c_{\phi - \tilde{\phi}} \frac{\Delta m^2_{21}}{\Delta m^2_{21} c^2_\omega - \lambda_-} - s_{\tilde{\phi}} s_{\phi - \tilde{\phi}} \frac{\Delta m^2_{21}}{\lambda_+ - \Delta m^2_{21} c^2_\omega} \right) \sin^2 \frac{\lambda_+ - \lambda_-}{4E} L \right] \\
&\quad + \frac{1}{4} s_\delta s_{2\psi} s_{2\omega} s_{2\tilde{\phi}} \left(c_{\tilde{\phi}} c_{\phi - \tilde{\phi}} \frac{\Delta m^2_{21}}{\Delta m^2_{21} c^2_\omega - \lambda_-} + s_{\tilde{\phi}} s_{\phi - \tilde{\phi}} \frac{\Delta m^2_{21}}{\lambda_+ - \Delta m^2_{21} c^2_\omega} \right) \\
&\quad \times \left(\sin \frac{\lambda_+ - \Delta m^2_{21} c^2_\omega}{2E} L + \sin \frac{\Delta m^2_{21} c^2_\omega - \lambda_-}{2E} L - \sin \frac{\lambda_+ - \lambda_-}{2E} L \right) \\
&\quad + 2 s^2_\psi s^2_{2\tilde{\phi}} \sum_n \mathrm{Re}[a_n] \frac{(\lambda_+ - \lambda_-) c_{2\tilde{\phi}}}{(\lambda_+ - \lambda_-)^2 - (2Ep_n)^2} \sin^2 \frac{\lambda_+ - \lambda_-}{4E} L.
\end{aligned} \tag{24}$$

From this equation (24) we find the following: (i) The matter profile effect is relevant when some of the Fourier coefficients a_n's are as large as Δm^2_{21} or the resonance condition [17],

$$\lambda_+ - \lambda_- = 2Ep_n, \tag{25}$$

is satisfied. (ii) The matter profile effect decreases in proportion to $1/n$ when the resonance condition is not satisfied. Therefore the higher Fourier modes are expected to be irrelevant. In other words, we do not need the details of the matter profile. Thus we expect that we can truncate the Fourier expansion of $a(x)$ at the finite number N. We can estimate the matter profile effect in neutrino factories.

III. NUMERICAL ANALYSIS

In this section we examine how many terms in the Fourier expansion are necessary. To see this we compare the oscillation probability and the event rate calculated using the PREM with those calculated using the truncated Fourier series (7). We first calculate the transition probabilities with several matter profiles, the PREM matter profile and the Fourier series matter profiles that are truncated at various N's. Next, using these probabilities we derive the event rates in the appearance channel, $\nu_e \to \nu_\mu$, as the ''observed'' numbers in an experiment. To derive them we use the following equation with a given number of muons in decay N_μ, muon energy E_μ, detector size N_{kt} and detection efficiency ϵ.

$$N_{\nu_e \to \nu_\mu} = \int_{E_{th}}^{E_\mu} \frac{dE}{E_\mu} \times \overbrace{\frac{N_\mu}{\pi L^2} \gamma^2 12 \left(\frac{E}{E_\mu} \right)^2 \left(1 - \frac{E}{E_\mu} \right)}^{flux} \times \overbrace{P_{\nu_e \to \nu_\mu}(E)}^{probability} \times \overbrace{\sigma_\nu(E) N_{kt} N_A \epsilon}^{detector}$$

where

$$\sigma_\nu = 0.67 \times 10^{-42} \times \left(\frac{E}{\mathrm{GeV}} \right) [m^2]$$

is the *CC* cross section, N_A's Avogadro's number, $\gamma \equiv E_\mu / m_\mu$, m_μ is the muon mass, and E_{th} is the threshold

energy of the detection. Then we compare these results. Through these comparisons we find how many Fourier coefficients we have to introduce to the theoretical parameters. In the following we assume that $N_\mu N_{kt}\epsilon = 5\times 10^{22}$ kt.[3]

A. $L = 3000$ km

Neutrino factories of this length are considered to be most efficient, so we consider this case first. The matter profile[4] and its Fourier coefficients are shown in Fig. 1. From these figures we find that the density fluctuation is very small. It should also be noted that the resonance condition (25) will not be satisfied for any n in neutrino factories. These facts indicate that the the constant matter density approximation is valid. In other words, the Fourier modes will be irrelevant. To confirm this we plot the oscillation probabilities in Fig. 2 with the various matter profiles: (i) constant density (dotted line), (ii) Eq. (7) with $N=1$ (dashed line), and (iii) PREM matter profile in Fig. 1 (solid line). We find that indeed this figure confirms our expectation.

The event rates are shown in Fig. 3. We plot the event rates calculated with the following δ's and the matter profiles: (i) $\delta=\pi/2$ and constant density (dotted line), (ii) $\delta=\pi/2$ and the PREM matter profile (solid line), and (iii) $\delta=0$ and the PREM matter profile (dash-dotted line). The event rate with $\delta=\pi/2$ is different from that with $\delta=0$.[5] We can observe this difference, if we know all the other theoretical parameters, the mixing angles, Δm^2's and $\overline{a}$ accurately enough.[6] Therefore we have to consider the contribution of δ to the oscillation probability. However, we cannot see the difference of the event rate for the case $a_1=0$ and $a_1\neq 0$ with baseline $L=3000$ km. Thus we do not have to take into account the fluctuation of the matter density.

B. $L = 7332$ km

There are many analyses of oscillation physics with the baseline length $L=7332$ km too. Therefore we consider this case next.

The matter profile based on the PREM and its Fourier coefficients are shown in Fig. 4. We find that the first two coefficients are large. We argue, however, that the first Fourier coefficient among them contributes much more to the oscillation probability because the resonance condition (25) for $n=\pm 1$ can be satisfied in a neutrino factory.

In Fig. 5, we compare the oscillation probabilities calculated with different matter profiles: (i) constant density (dot-

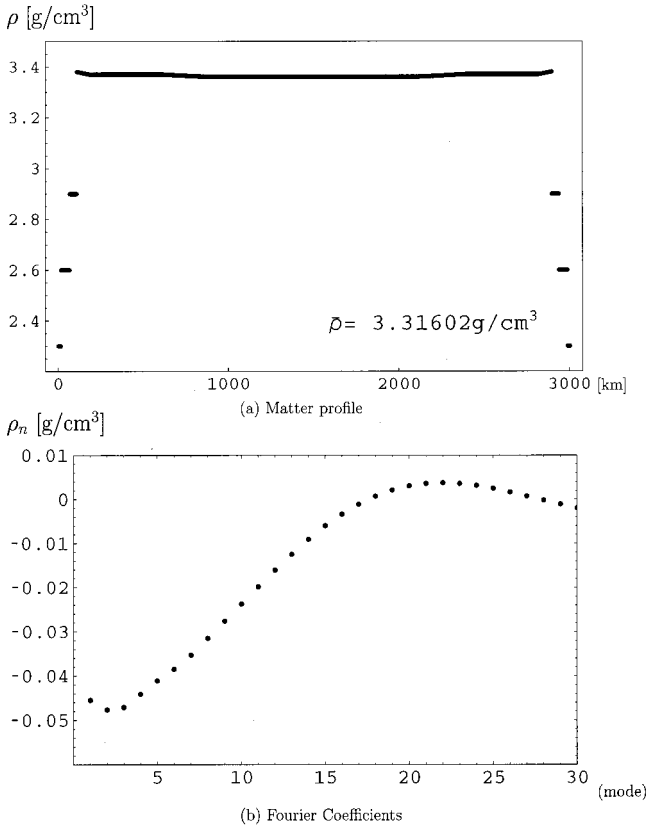

FIG. 1. (a) Matter profile on the baseline and (b) its Fourier coefficients for $L=3000$ km.

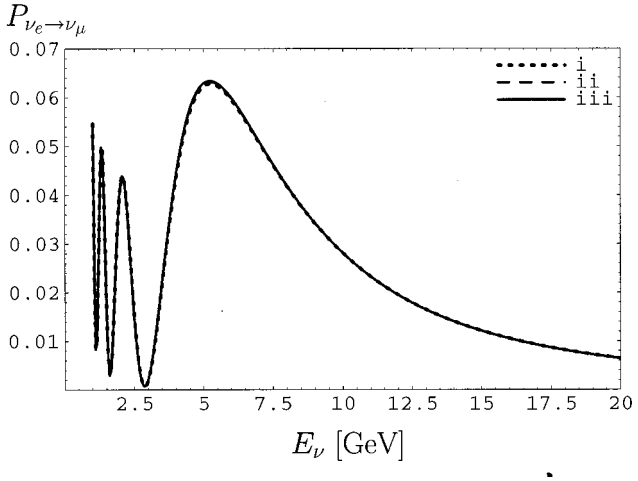

FIG. 2. Transition probability $P_{\nu_{e\to\nu_\mu}}$ for $L=3000$ km. In this plot we set $\sin\omega=1/\sqrt{2}$, $\sin\psi=1/\sqrt{2}$, $\sin\phi=0.1$, $\Delta m^2_{31}=3\times 10^{-3}$ eV^2, $\Delta m^2_{21}=5\times 10^{-5}$ eV^2, $\overline{a}=2.51\times 10^{-4}(E_\nu/[\mathrm{GeV}])$ eV^2, $a_1=-3.44\times 10^{-6}(E_\nu/[\mathrm{GeV}])$ eV^2, and $\delta=\pi/2$. There are three lines corresponding to the following matter profiles: (i) constant density (dotted line), (ii) Eq. (7) with $N=1$ (dashed line), and (iii) PREM matter profile in Fig. 1 (solid line). These lines are quite similar to each other so that we cannot see these three lines individually.

[3]We also assume that we can reconstruct the neutrino energy.

[4]To calculate the matter profile, we linearly interpolate the PREM's data given discretely for the depth. For this calculation we modify the density of the crust (or the most outside layer) into 2.3 g/cm^3 from 1 g/cm^3.

[5]In this paper, we consider the cases $\delta=\pi/2$ and $\delta=0$ to study whether we can see the pure *CP* violation effect. Though there is no *CP* violation effect for $\delta=\pi$ [18], for simplicity we compare only these two cases.

[6]We cannot see this difference, however, since we will not determine the theoretical parameters accurately enough [18].

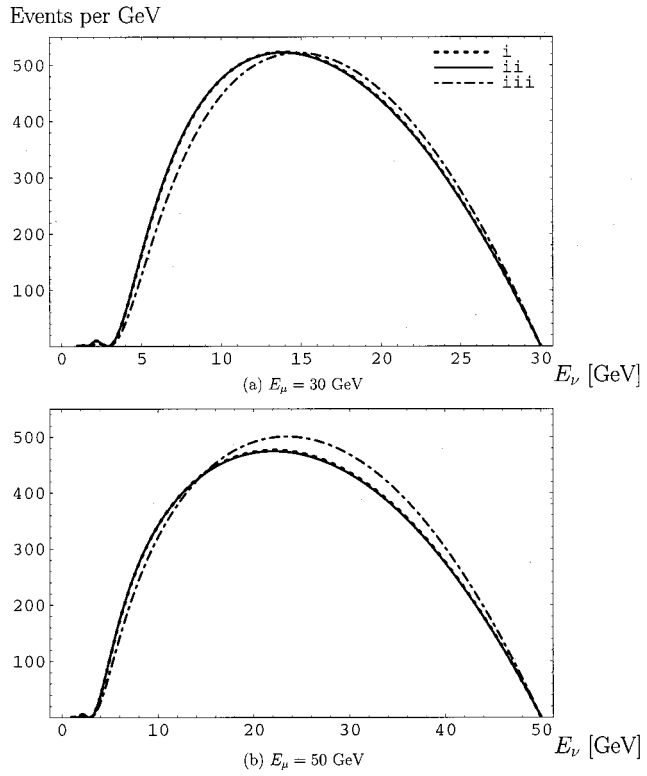

FIG. 3. Differential event rate $N_{\nu_e \to \nu_\mu}$ for $L = 3000$ km with (a) $E_\mu = 30$ GeV and (b) $E_\mu = 50$ GeV. The oscillation parameters are same as those in Fig. 2 except δ. There are three lines with respect to δ and the following matter profiles: (i) $\delta = \pi/2$ and constant density (dotted line), (ii) $\delta = \pi/2$ and PREM matter profile (solid line), and (iii) $\delta = 0$ and PREM matter profile (dash-dotted line). Curve line (iii) is different from the others.

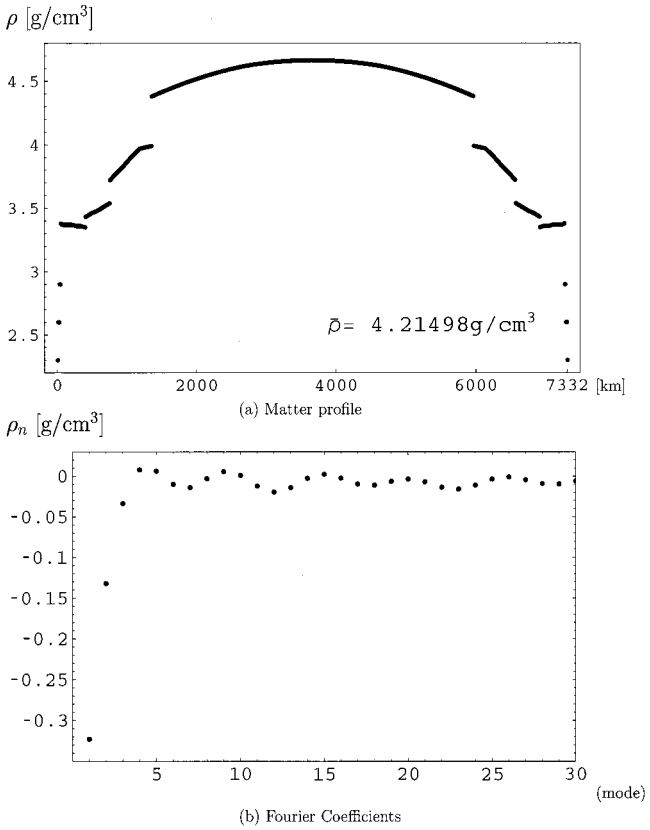

FIG. 4. (a) Matter profile on the baseline and (b) its Fourier coefficients for $L = 7332$ km.

ted line), (ii) Eq. (7) with $N = 1$ (dashed line), (iii) Eq. (7) with $N = 2$ (dash-dotted line), and (iv) the PREM matter profile in Fig. 4 (solid line).

We see that the probability calculated using PREM [Fig. 5, profile (iv)] and another calculated using Eq. (7) with $N = 1$ [Fig. 5, profile (ii)] are very similar. However the probability calculated using the constant density matter profile [Fig. 5, profile (i)] is quite different. Furthermore, there is no significant difference between the probabilities calculated using Eq. (7) with $N = 1$ and $N = 2$ [Fig. 5, profiles (ii) and (iii)]. Thus we have to take into account a new parameter a_1 in the analysis of neutrino factories with the baseline $L = 7332$ km. This new parameter a_1 should be estimated by the experimental results.

To see the importance of a_1 more clearly, we show the event rate in Fig. 6 using different δ and different matter profiles: (i) $\delta = \pi/2$ and the constant density approximation (dotted line), (ii) $\delta = \pi/2$ and the matter profile (7) with $N = 1$ (dashed line), (iii) $\delta = \pi/2$ and the PREM matter profile (solid line), and (iv) $\delta = 0$ and the PREM matter profile (dash-dotted line).

The distributions of the event rate in Fig. 6, profiles (i) and (iii) are quite different from each other. This means that the estimation of the event rate with the constant density approximation does not work. In other words, we cannot estimate the values of the parameters from the experimental

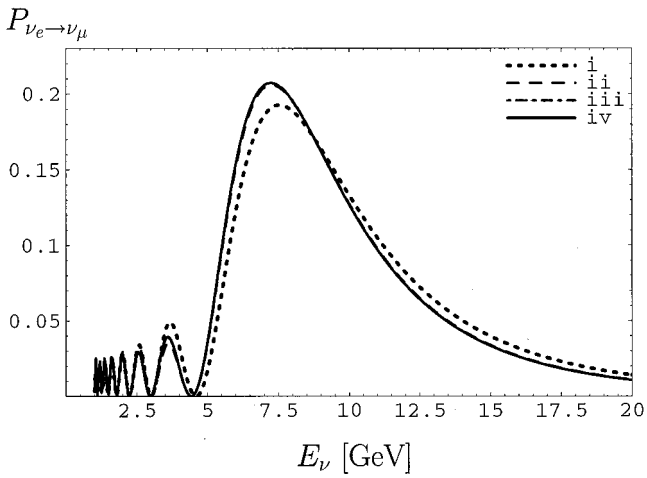

FIG. 5. Transition probability $P_{\nu_e \to \nu_\mu}$ for $L = 7332$ km. The oscillation parameters are the same as those in Fig. 2 but $\bar{a} = 3.19 \times 10^{-4} (E_\nu/[\text{GeV}])\ \text{eV}^2$, $a_1 = -2.44 \times 10^{-5} (E_\nu/[\text{GeV}])\ \text{eV}^2$, and $a_2 = 9.98 \times 10^{-6} (E_\nu/[\text{GeV}])\ \text{eV}^2$. There are four lines corresponding to the following matter profiles; (i) constant density (dotted line), (ii) Eq. (7) with $N = 1$ (dashed line), (iii) Eq. (7) with $N = 2$ (dash-dotted line), and (iv) PREM matter profile in Fig. 4 (solid line). Curve (i) is quite different form the others, while the other three lines show quite a similar line shape.

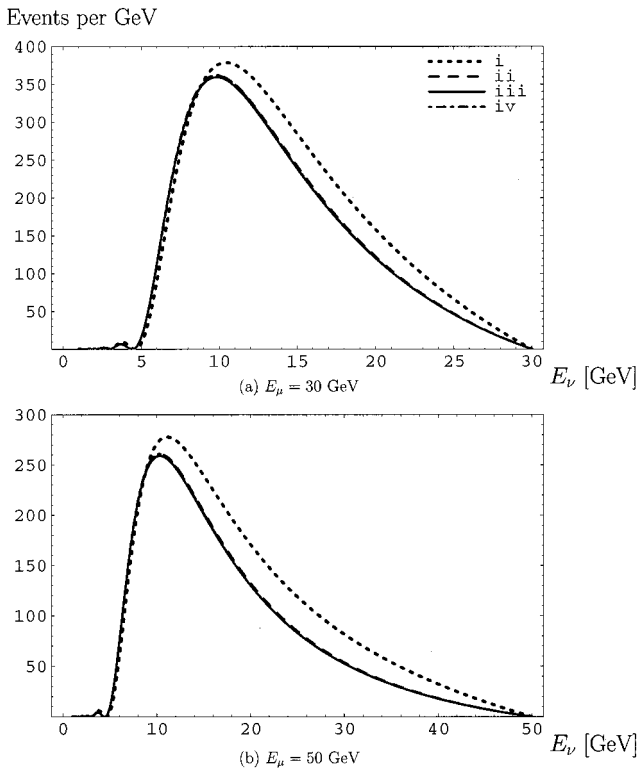

FIG. 6. Differential event rate $N_{\nu_e \to \nu_\mu}$ for $L = 7332$ km with (a) $E_\mu = 30$ GeV and (b) $E_\mu = 50$ GeV. The oscillation parameters are the same as those in Fig. 2 except δ. There are four lines with respect to δ and the following matter profiles: (i) $\delta = \pi/2$ and constant density (dotted line), (ii) $\delta = \pi/2$ and Eq. (7) with $N = 1$ (dashed line), (iii) $\delta = \pi/2$ and PREM matter profile (solid line), and (iv) $\delta = 0$ and PREM matter profile (dash-dotted line). Curve (i) is different from the others while the other three are quite similar.

data precisely without taking into account the contribution of a_1. On the other hand, the event rates in profiles (ii) and (iii) are quite similar. If we can insist from Fig. 3 that we can observe the *CP* violating effect, then we can insist from Fig. 6 that we can observe the effect of a_1. Furthermore, since the contribution of a_1 cannot be explained by other terms, we expect that we can estimate a_1 very well experimentally. We can study geophysics by neutrinos.

Consider the difference between profiles (iii) and (iv) in Fig. 6. The effect of the *CP* violating phase on the event rate is so small that we cannot distinguish between the two theories that have different *CP* violating phases. Indeed the effect of δ is smaller than that of a_2, which is already beyond the experimental sensitivity.

C. $L = 12\,000$ km

In this case neutrinos penetrate the Earth almost along its diameter. Neutrinos go through both the mantle and the core. Therefore the matter profile is very complicated. We expect that we can observe the higher modes in Eq. (7).

The matter profile and the Fourier coefficients are given in Fig. 7. From these figures we expect that not only a_1 but also the higher Fourier modes are relevant.

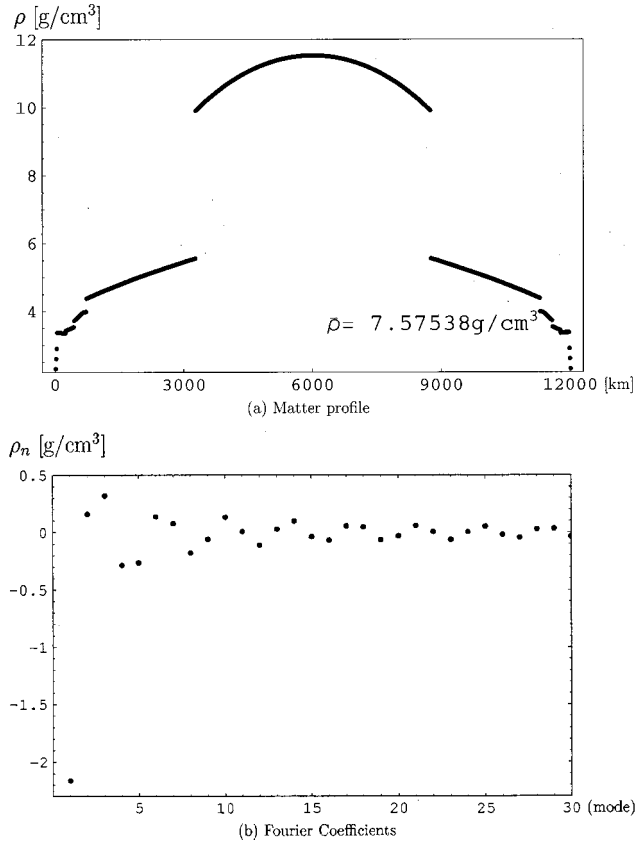

FIG. 7. (a) Matter profile on the baseline and (b) its Fourier coefficients for $L = 12\,000$ km.

In Fig. 8, we plot the transition probabilities corresponding to the matter profiles (i) constant density (dotted line), (ii) Eq. (7) with $N = 1$ (dashed line), (iii) Eq. (7) with $N = 3$ (dash-dotted line), and (iv) the PREM matter profile in Fig. 7 (solid line). From Fig. 8 we find that there are significant contributions to the oscillation probability from the higher modes. The probability calculated with the constant density matter profile [Fig. 8, profile (i)] is quite different from that calculated with the PREM matter profile [Fig. 8, profile (iv)]. Even the probability calculated using the matter profile, Eq. (7), with $N = 1$ [Fig. 8, profile (ii)] differs apparently from that with the PREM matter profile [Fig. 8, profile (iv)]. On the other hand, we find that the matter profile, Eq. (7), with $N = 3$ mimics very well the PREM matter profile to calculate the oscillation probability.

We also plot the event rates in Figs. 9. There the lines correspond to the following δ and matter profiles: (i) $\delta = \pi/2$, Eq. (7), with $N = 1$ (dotted line), (ii) $\delta = \pi/2$, Eq. (7), with $N = 3$ (dashed line), (iii) $\delta = \pi/2$ and PREM matter profile (solid line); (iv) $\delta = 0$ and PREM matter profile (dash-dotted line). We see few discrepancies in profiles (ii), (iii), and (iv) in Fig. 9, while there is a conceivable difference between profile (i) and the others in Fig. 9. We find, therefore, that the effect of δ is irrelevant in the oscillation physics, while the first three modes of the Fourier coefficients have a measurable contribution to the oscillation physics.

We examine more carefully whether the higher mode contribution is really measurable. The number of the necessary

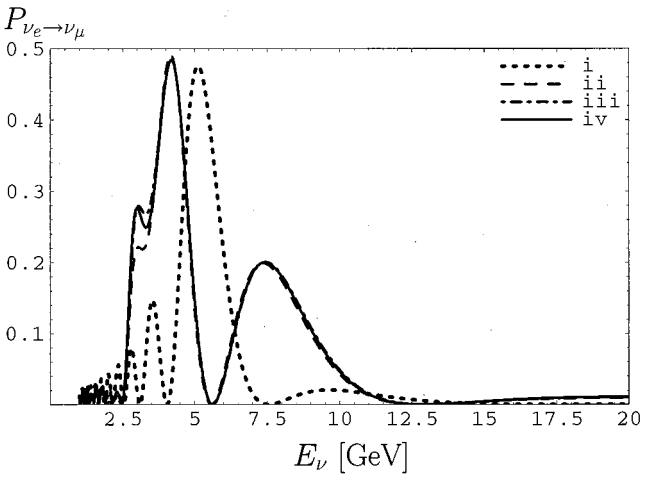

FIG. 8. Transition probability $P_{\nu_e \to \nu_\mu}$ for $L=12\,000$ km. In this plot we use the same oscillation parameters as those in Fig. 2 but $\bar{a}=5.73\times10^{-4}(E_\nu/[\mathrm{GeV}])\ \mathrm{eV}^2$, $a_1=-1.63\times10^{-4}(E_\nu/[\mathrm{GeV}])\ \mathrm{eV}^2$, $a_2=1.21\times10^{-5}(E_\nu/[\mathrm{GeV}])\ \mathrm{eV}^2$, and $a_3=2.42\times10^{-5}(E_\nu/[\mathrm{GeV}])\ \mathrm{eV}^2$. There are four lines corresponding to the following matter profiles: (i) constant density (dotted line), (ii) Eq. (7) with $N=1$ (dashed line), (iii) Eq. (7) with $N=3$ (dash-dotted line), and (iv) PREM matter profile in Fig. 7 (solid line). Curve (i) is quite different from the others. Curve (ii) is also different from the curve (iv), while curve (iii) shows quite a similar shape with curve (iv).

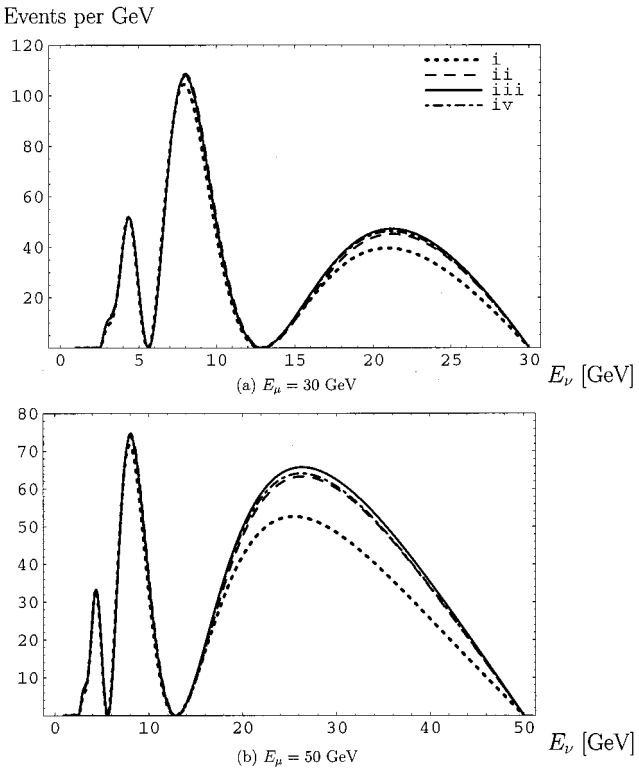

FIG. 9. Differential event rate $N_{\nu_e \to \nu_\mu}$ for $L=12\,000$ km with (a) $E_\mu=30$ GeV and (b) $E_\mu=50$ GeV. The oscillation parameters are the same as those in Fig. 2 except δ. There are four lines corresponding to δ's and the matter profiles: (i) $\delta=\pi/2$ and Eq. (7) with $N=1$ (dotted line), (ii) $\delta=\pi/2$ and Eq. (7) with $N=3$ (dashed line), (iii) $\delta=\pi/2$ and PREM matter profile (solid line); (iv) $\delta=0$ and PREM matter profile (dash-dotted line).

new parameters is quite dependent on the event rate of the experiment. We can find that there is a conceivable difference between profile (i) and profiles (ii) and (iii) in Fig. 9. However, this difference is not significant statistically in Fig. 9(a). As long as $N_\mu N_{kt}\epsilon$ is less than 5×10^{22}, we need to introduce only a_1 as the theoretical parameter. On the other hand, this discrepancy is very significant in Fig. 9(b). We can measure the contributions from the higher modes such as a_2 and a_3. We should introduce higher modes according to the expected event rate.

IV. SUMMARY AND DISCUSSION

We considered how to deal with the matter profile effect. We proposed that the Fourier coefficients of the matter profile are used as the theoretical parameters. Using this method we can evaluate the size of the ambiguities in the estimate of the mixing parameters.

The perturbative solution for the evolution equation, Eq. (24), implies that the higher Fourier modes are irrelevant. The introduction of the first few modes gives enough precision to the estimate of the event rate.

We saw the following three cases in detail numerically.

$L=3000$ km. The matter profile effect itself is irrelevant. We can assume the matter density is constant.

$L=7332$ km. We need to introduce a_1 as the theoretical parameter that should be measured experimentally. On the other hand, the *CP* violating phase δ is irrelevant. We cannot determine the *CP* violating phase at this baseline.

$L=12\,000$ km. We need to introduce higher modes as the theoretical parameters. However, since the event rate with this baseline length is significantly small, by using only a_1 we can estimate the theoretical parameters accurately within the precision of the experiment. Depending on the precision required, we must decide the number of coefficients to introduce.

In general the Fourier modes are relevant when the baseline passes through the lower mantle ($L\gtrsim5000$ km). In this case we need to use the method developed in this paper to make an accurate analysis. In other words, we can explore the interior of the earth in neutrino factories.

ACKNOWLEDGMENTS

The authors are grateful to K. Harada and M. Koike for useful discussions. The work of J.S. is supported in part by a Grant-in-Aid for Scientific Research of the Ministry of Education, Science and Culture, No. 12047221 and No. 12740157.

[1] Super-Kamiokande Collaboration, Y. Fukuda *et al.*, Phys. Rev. Lett. **81**, 1562 (1998).
[2] For example, see K. Nishikawa, Report No. INS-Rep-924, 1992; S. Parke, Report No. Fermilab-Conf-93/056-T, 1993; hep-ph/9304271; see also http://cupp.oulu.fi/neutrino/
[3] S. Geer, Phys. Rev. D **57**, 6989 (1998); **59**, 039903 (1999).
[4] V. Barger, S. Geer, and K. Whisnant, Phys. Rev. D **61**, 053004 (2000).
[5] A. Cervera, A. Donini, M. B. Gavela, J. J. Gomez Cadenas, P. Hernandez, O. Mena, and S. Rigolin, Nucl. Phys. **B579**, 17 (2000).
[6] V. Barger, S. Geer, R. Raja, and K. Whisnant, Phys. Rev. D **62**, 013004 (2000); **62**, 073002 (2000); Phys. Lett. B **485**, 379 (2000); Phys. Rev. D **63**, 033002 (2001).
[7] A. De Rujula, M. B. Gavela, and P. Hemandez, Nucl. Phys. **B547**, 21 (1999); A. Donini, M. B. Gavela, P. Hernandez, and S. Rigolin, *ibid.* **B574**, 23 (2000).
[8] K. Dick, M. Freund, M. Lindner, and A. Romanino, Nucl. Phys. **B562**, 29 (1999); A. Romanino, *ibid.* **B574**, 675 (2000); M. Freund, M. Lindner, S. T. Petcov, and A. Romanino, *ibid.* **B578**, 27 (2000).
[9] M. Freund, P. Huber, and M. Lindner, Nucl. Phys. **B585**, 105 (2000).
[10] Neutrino Factory and Muon Collider Collaboration, K. T. McDonald, physics/9911009; C. Albright *et al.*, hep-ex/0008064.
[11] M. Campanelli, A. Bueno, and A. Rubbia, hep-ph/9905240; A. Bueno, M. Campanelli, and A. Rubbia, Nucl. Phys. **B573**, 27 (2000); **B589**, 577 (2000).
[12] M. Koike and J. Sato, Phys. Rev. D **61**, 073012 (2000).
[13] O. Yasuda, hep-ph/0005134.
[14] L. Wolfenstein, Phys. Rev. D **17**, 2369 (1978); V. Barger, R. J. N. Phillips, S. Pakvasa, and K. Whisnant, *ibid.* **22**, 2718 (1980); S. P. Mikheev and A. Yu. Smirnov, Yad. Fiz. **42**, 1441 (1985) [Sov. J. Nucl. Phys. **42**, 913 (1985)].
[15] A. M. Dziewonski and D. L. Anderson, Phys. Earth Planet. Inter. **25**, 297 (1981).
[16] M. Koike and J. Sato, Mod. Phys. Lett. A **14**, 1297 (1999).
[17] P. I. Krastev and A. Yu. Smirnov, Phys. Lett. B **226**, 341 (1989).
[18] M. Koike, T. Ota, and J. Sato, hep-ph/0011387.